SDF-1/CXCR4 Axis-mediated Migration of Systematically Transplanted Bone Marrow Mesenchymal Stem Cells Towards the Injured Spinal Cord in a Rat Model

Sa Cai (caisa@szu.edu.cn)
Shenzhen University

Yi Yang
Health Science Center, Shenzhen University, Shenzhen, China

Andong Zhao
Health Science Center, Shenzhen University, Shenzhen, China

Yu Pan
Department of Trauma and Orthopedics, The 2nd Affiliated Hospital of Shenzhen University, The Affiliated Baoan Hospital of Southern Medical University, Shenzhen, China

---

Research

Keywords: bone marrow mesenchymal stem cells, spinal cord injury, migration, SDF-1, CXCR4

Posted Date: September 8th, 2020

DOI: https://doi.org/10.21203/rs.3.rs-70771/v1

Abstract

Background: Bone marrow-derived mesenchymal stem cells (MSCs) have been shown to migrate to injured spinal cords and promote functional recovery when systemically transplanted into the traumatized spinal cord. However, the the mechanisms underlying their migration to spinal cords are not yet fully understood

Methods: In this study, we systemically transplanted GFP- and luciferase-expressing MSCs into the rat models of spinal cord injury and examined the role of the stromal cell-derived factor 1 (SDF-1)/CXCR4 axis in regulating the migration of transplanted MSCs to spinal cords.

Results: After intravenous injection, MSCs migrated to the injured spinal cord where the expression of SDF-1 was increased. Spinal cord recruitment of MSCs was blocked by pre-incubation with an inhibitor of CXCR4. Their presence correlated with morphological and functional recovery. In vitro, SDF-1 or cerebrospinal fluid (CSF) collected from SCI rats promoted a dose-dependent migration of MSCs, which was blocked by an inhibitor of CXCR4 or an SDF-1 antibody.

Conclusions: The study suggests that SDF-1/CXCR4 interactions recruit exogenous MSCs to injured spinal cord tissue and may enhance neural regeneration. Modulation of homing capacity may be instrumental in harnessing the therapeutic potential of MSCs.

Background

Mesenchymal stem cells (MSCs) represent a promising source of cells for tissue repair because they are multipotent, easy for isolation and expansion in vitro, and lack of the promotion of immuno-rejection [1, 2]. Much evidence shows that MSCs can home to tissues, particularly when injured or under pathological conditions [3]. For example, MSCs can migrate to damaged tissues, including bone or cartilage fracture [4, 5], liver injuries [6], acute lung injuries [7], myocardial infarctions [8], nerve injuries [9–12], and skins [13]. Apart from differentiating into functional cells for tissue reparation after location, MSCs, themselves, secrete a broad spectrum of bioactive macromolecules that are both immunoregulatory and serve to regenerative microenvironments in fields of tissue injury [2, 14]. Therefore, MSCs appear to be valuable mediators for tissue repair and regeneration.

Although the mechanisms by which MSCs home to tissues and migrate across the endothelial cell layer are not yet fully understood, it is likely that chemokines and their receptors, as well as adhesion molecules, are involved, as they are important factors known to control cell migration [15, 16]. Among them, the predominant role of the chemokine, stromal-cell-derived factor 1 (SDF-1) and its receptor C-X-C chemokine receptor type 4 (CXCR4) expressed on MSCs is now well-established [17]. SDF-1 is constitutively expressed in a wide range of tissues, including the central nervous system [15, 18–20].

Natural chemo-attractive mechanisms can bring MSCs from far sites and near to sites of tissue damage to establish reparative/regenerative microenvironments. Clearly, by direct delivery or manipulative

targeting of MSCs to sites of tissue injury, we could profoundly control the extent of damage, cell death, and subsequent regeneration of various tissues. Herein, we investigated the homing of bone marrow-derived MSCs to the site of spinal cord injury (SCI), which will lay the foundation for MSC-based therapy of SCI.

Methods

Animals

GFP transgenic rats (Japan SLC, Inc.; Hamamatsu, Japan) and Sprague-Dawley (SD) wild-type rats, genetically identical to each other except for their transgenes, were used. All experimental procedures employed in this study have been approved by Institutional Animal Care and Use Committees of Shenzhen University.

Culturing of mesenchymal stem cells

Bone marrow-derived MSCs were harvested from GFP transgenic rats according to the procedure described previously [21]. Briefly, after the sacrifice of the animal, the femur and tibia were removed and flushed out with phosphate-buffered saline (PBS). The marrow was collected and spun down, the supernatant discarded, and the resulting cell pellet suspended in Dulbecco's modified Eagle's medium (DMEM; Gibco, USA) with 10% fetal bovine serum (Biosera, UK) and antibiotics (100IU/ml penicillin G and 100 μg/ml streptomycin), namely MSC culture medium, and transferred to tissue culture flasks (Costar, USA) at densities ranging from $1\times 10^5/cm^2$ to $1\times 10^6/cm^2$. Cultures were incubated at 37°C in 5% CO_2. The medium was changed after 48 h and then every 2 to 3 days. Primary cultures were maintained for 7 to 10 days, during which time the non-adherent hematopoietic cell fraction was depleted. After the cells had grown to near confluence, they were passaged 2 to 3 times by digestion with 0.25% trypsin and 0.02% EDTA.

Lentiviral vectors and MSC transfection

The lentiviruses were created using the ViraPower™ Lentiviral Expression System (Invitrogen, Paisley, UK). The coding sequence of luciferase was subcloned into pLenti6/V5-D-TOPO (Invitrogen). pLenti6/V5-DTOPO/luciferase vector and the ViraPower™ Packaging Mix (Invitrogen) were co-transfected using a gene carrier kit (Epoch-Biolabs, Missouri City, TX, USA) into the 293T cell line to produce a lentiviral stock. Forty-eight hours post-transfection, virus-containing supernatant was harvested by collecting the medium. Viral particles were purified by ultracentrifugation through a 20% sucrose cushion. For infecting MSC, cells were cultured in 24-well plates, and when the culture reached 80% confluence, the concentrated lentivirus was added to the culture dishes. After incubation for 48 h, the medium was replaced with selection medium containing 10 μg/ml blasticidin. The selection medium was replaced

every 2 days until antibiotic-resistant colonies were identified, and thus a stable cell line of MSC-GFP-Luci was established.

In vitro firefly luciferase assays

Cells were dislodged from culture flasks to be resuspended in PBS. Cell suspensions were divided into a 96-well plate in known concentrations. After administration of D-Luciferin (4.5 μg/ml, Goldbio, USA), peak signal expressed as photons per second per centimeter square per steridian (photons/s/cm^2/sr) was measured using a charged coupled device camera (IVIS100, Xenogen, Alameda, CA, USA). All samples were conducted in triplets.

Spinal cord injury (SCI) and postoperative care

Eighty-three male SD rats (240 to 260 g) were used for visualizing the location of transplanted MSCs-GFP-Luci on the whole spinal cord. The lesion induction and cellular transplantation were standardized. Under anesthesia with pentobarbital sodium (50 mg/kg, ip), contusion injury was performed at the mid-thoracic (T8-T9) level of the spinal cord. A standard spinal cord contusion was made using a weight-drop device. A metal rod 8 g in weight and 2.0 mm in diameter was dropped from a height of 10 mm onto the exposed spinal cord for contusion injury. Sixty-nine rats were used for MSCs-GFP-Luci transplantation, and the remaining 14 rats served as controls. Sixty-nine rats for transplantation were divided into three groups: 23 rats were treated with MSCs, 23 rats with the injection of SDF-1 followed by transplantation of MSCs, and the other 23 rats with AMD3100-pretreated MSCs. The control rats were treated with PBS. 3 rats of each experimental group were performed in vivo fluorescence imaging at time points of 1, 3, 5, 7, 11, and 14 days after cell injection, 14 rats were performed RT-PCR and western blotting, while the other 6 rats were respectively undergone transcardiac perfusion with a fixative containing 4% paraformaldehyde in 0.1 M phosphate buffer.

For the rats pretreated with SDF-1, a Hamilton syringe needle was inserted into the spinal cord to a depth of 2 mm from the surface of the dura mater at a point 3 mm rostral to the injury site, and 5 μl of SDF-1 (500ng/ml) were introduced into the spinal cord over 5 min with an automatic microinjection pump (Muromachi Kikai Co., Tokyo, Japan).

Animals received continuous attention after surgery. Weight control was performed daily. Bladder expression was performed per day until reaching a maximum of 2 ml of urine in the morning expression, or the animal recovered its bladder function. Urine volume, PH, and blood presence were also monitored. Urinary tract infections were treated with the suspension of cefazolin and administration of 12 mg/kg gentamicin for 1 week. Ascorbic acid (60 mg/ml; Merk, Germany) was administered to prevent bacterial growth. Animals were examined daily for signs of autophagia, and treated with acetaminophen 64 mg/kg (baby Tylenol, McNeil, USA) for 1 week to stop self-mutilation.

Cerebrospinal fluid (CSF) collection

For rats, CSF was collected before and 24, 48, 72, 96, and 120 h after SCI. Prior to CSF collection, the fur on the neck region of the rat was removed and anesthetized with 5% halothane. A needle connected to a syringe was inserted horizontally and centrally into the cisterna magna for CSF collection without making any incision at this region. A gentle aspiration will make the CSF flow through the needle. The colorless CSF sample is slowly drawn into the syringe, and the color of the CSF was carefully observed to avoid any possible blood contamination. The non-contaminated sample was drawn into the syringe.

SDF-1 in CSF was measured by enzyme-linked immunosorbent assay (ELISA) with commercial kits (R&D System, USA) and western blotting. ELISA was carried out according to the manufacturer's recommendations.

For western blotting, the collected CSF or tissue sample was lysed with lysing buffer (Sigma-Aldrich). Protein concentration was measured using the Bradford protein assay. Proteins were denatured by boiling for 3 min in the presence of β-mercaptoethanol. Equal amounts of protein were separated by SDS-PAGE and transferred to polyvinylidene difluoride membrane (Millipore Corp., Bedford, MA, USA). Membranes were blocked in TBST containing 5% nonfat milk at room temperature for 2 h and probed with the rabbit anti-rat polyclonal primary antibody directed against SDF-1 (Santa Cruz, CA) overnight at 4˚C. Then the membranes were blotted with horseradish peroxidase (HRP)-linked mouse anti-rabbit IgG (Bio-Rad, Hercules, CA). β-actin was shown as a control. Proteins were visualized by using Kodak film (Kodak, Rochester, USA)

Cell transplantation and in vivo bioluminescence imaging (BLI)

The experimental rats were randomly divided depending on their treatment after thoracic SCI. For transplantation group, MSCs-GFP-Luci were trypsinized with 0.25 M EDTA and 0.05% trypsin (Invitrogen) on the day of transplantation and resuspended in PBS at 1×10^{7} cells/ml; 1×10^{6} of cells were injected into the tail vein of SCI-rats. The animals were examined at different time points after the injection using the imaging system (IVIS100, Xenogen). For each time, D-luciferin was dissolved in PBS and given to each rat by intraperitoneal injection at a dose of 150 mg/kg. Rats were imaged 5 min later using a 20-cm field of view and an exposure time of 3 min (3 min exposure; f-stop, 1; binning, 16; the field of view, 15 cm). Bioluminescence values were calculated by measuring photons/s/cm^2/sr in the region of interest (ROI). For the control group, the rats received an injection of PBS, the amount of which was similar with that of the transplanted MSC group.

Histological Analysis

Histological evaluation was performed at the time points of the different groups in the experiment. The animals were killed at 1, 3, 7, 14, and 21 days after transplantation surgery. The T8-10 portion of the spinal cord was removed from the vertebral column and was then immersed for 24 h in the fixative containing 4% paraformaldehyde. The tissue was embedded in paraffin and sectioned sagittally (6 μm thickness). All sections were stained with hematoxylin-eosin (HE) for general histology. For assessment of the distribution of transplanted MSCs-GFP-Luci, the fluorescence emitted by GFP was directly observed by fluorescence microscopy (BX51; Olympus Optical, Tokyo, Japan).

Transwell migration assay

The migratory ability of MSCs-GFP-Luci was determined using transwell plates (Corning Costar, Cambridge, MA) that were 6.5mm in diameter with 8 μm pore filters. In brief, cells were suspended in serum-free medium and seeded into the upper well, and different concentrations of SDF-1-containing medium or different concentrations of CSF-containing medium were placed in the lower well of a transwell plate. Following incubation for 4 h at 37^{o}C, cells that had not migrated from the upper side of the filter were scraped off with a cotton swab, and those in the lower surface were fixed with 95% ethanol, stained with hematoxylin. The number of cells that had migrated to the lower side of the filter was counted under a light microscope at 200 magnification in five randomly-selected fields. Each experiment was performed in triplicate. Where indicated, cells were incubated with AMD3100 blocking against CXCR4 or the antibody against SDF-1 (Sigma). Serum-free medium was used as an experimental control.

RT-PCR

Total RNA was extracted with Trizol reagent (Invitrogen). Equal amounts of mRNA were subjected to RT-PCR analysis using a SuperScriptTM One-step RT-PCR kit (Invitrogen) according to the manufacturer's instructions. The endogenous gene glyceraldehyde-3-phosphate dehydrogenase (GAPDH) was also quantified to normalize differences in the added RNA and efficiency of reverse transcription. Following oligonucleotide primers were used: SDF-1 (AF189724), forward 5'-CCCTGCCGATTCTTTGAG-3', reverse 5'-GTCCTTTGGGCTGTTGTG-3'; GADPH (NM002406), forward 5'-CCA CAGTCCATGCCATCACTG-3', reverse 5'-CGCTGTTGAAGTCAGAGGAGA-3'; CXCR4 (AF452185), forward 5'-GGCAATGGGTTGGTAATC-3', reverse 5'-GACAATGGCAAGGTAGCG-3'. 1 μg of total RNA was reverse transcribed to synthesize cDNA at 50˚C for 30 min, and then the cDNA was subjected to PCR amplification with specific primers in 25μl mixtures. The amplification conditions were 30 cycles at 94˚C for 30 sec, 56˚C for 30 sec, and 72˚C for 45 sec in each cycle using an MJ PCR System. The PCR products were electrophoresed in a 2% agarose gel. All results represented the average density of positive bands obtained from 3 independent experiments.

Behavioral testing

The rats were tested behaviorally to evaluate the effect of MSCs-GFP-Luci on the recovery of motor function of the injured rats. Behavioral testing was performed for each limb using the Basso-Beatie-Bresnahan (BBB) locomotor rating scale at different time points (before the injury and on day 1, 7, 14, 21, 28 post-injury). For BBB assessment, rats were placed in an open field. Hindlimb motor function was scored simultaneously by two independent observers who were blind to the transplantation status of the animals. A 0 score represents no locomotion, and a 21 score represents a normal motor function. The scores for the left and right leg were averaged to generate the actual score for each trial.

Statistical analysis

All experiments were repeated at least three times unless otherwise indicated. Data are presented as mean±SD. Statistical analysis involved the use of the Student t-test. A $P<0.05$ was considered significant.

Results

Cell characterization of rat MSCs-GFP-Luci

Cultured rat MSCs-GFP-Luci had a fibroblast-like morphology (Figure 1A). They grew slowly for the first 5 days, then proliferated rapidly and gradually formed colonies with fine edges (Figure 1B). Cells were observed for GFP expression directly under a fluorescent microscope (Figure 1C). Luciferase imaging of MSCs-GFP-Luci at different cell concentration (100, 500, 1000, 5000, 10000, 15000, 20000, and 30000 per well) is shown using IVIS^{TM} (Xenogen) (Figure 1D). Cells produced in vitro a luciferase activity and cell number showed well correlation with luciferase signal on BLI (Figure 1E).

Expression of SDF-1 in the injured spinal cords

Total RNA and protein were extracted from spinal cord tissue in the control group on days 0, 1, 3, 5, 7, 11, 14 after surgery operation (n=2 for each time point). RT-PCR and western blotting analysis analyzed the expression levels of SDF-1 mRNA and protein (Figure 2A and 2B). SDF-1 expression increased in the injured tissue on day 1. Expression further increased on day 3 and maintained a constant level for the following days and then subsided after day 14. This result indicates the involvement of SDF-1 in the acute phase of SCI.

Expression of CXCR4 in spinal cords after transplantation of MSCs-GFP-Luci

RT-PCR analysis revealed an increase in CXCR4 mRNA expression in the injured spinal cords on day 3 after only transplantation of MSCs-GFP-Luci (Figure 3A and 3D). The expression levels markedly increased on day 5 and maintained a significant level for about 10 days (Figure 3A and 3D). On day 11,

the mRNA expression became weak and further decreased on day 14 (Figure 3A and 3D). This result indicated the proficient reaction of the exogenous stem cells to SDF-1 released from the injured tissue.

Expression of CXCR4 in the injured spinal cords after the pretreatment of SDF-1 and transplantation of MSCs-GFP-Luci

To investigate the effect of SDF-1, the SDF-1 had been injected into the injured spinal cord before the transplantation of MSCs-GFP-Luci. The expression of CXCR4 mRNA in the injured spinal cords was examined again. Its expression level was significantly elevated, starting on day 3 and continuing through the following days (Figure 3B and 3D). On day 14, the expression maintained the level higher than the group without pre-injection of SDF-1 (Figure 3D). Therefore, additional SDF-1 treatment could improve MSC migration in vivo.

Expression of CXCR4 in the injured spinal cords after transplantation of AMD3100-preincubated MSCs-GFP-Luci

To functionally confirm whether the SDF-1/CXCR4 axis plays an essential role in mediating MSC migration in vivo, AMD3100, a CXCR4-specific antagonist, was utilized in the study. AMD3100 at concentrations ranged from 1 to 10 μg/ml did not affect cell proliferation and survival, but exhibited a strong inhibitory effect on MSC migration in vivo when used at 5 μg/ml (Figure 3C and 3D). Before implantation, the serum-starved MSCs were pre-incubated with AMD3100 (5 μg/ml for 30 min at 37^{o}C). After their systematical injection into the SCI rats, the expressions of CXCR4 mRNA were much weaker compared with the previous groups (Figure 3C and 3D), suggesting that these AMD3100-pretreated cells scarcely migrated to the injured site. Thus, the pretreatment with the CXCR4-specific antagonist AMD3100 could significantly prevent the migration of MSCs to the injured spinal cord.

SDF-1 level in the CSF of SCI rat

SDF-1 was detectable in CSF of rats after SCI by western blotting and ELISA and analysis (Figure 4A and 4B). The CSF level of SDF-1 was increased at 48 hours after injury. A clear elevation was observed at 72 hours after injury (Figure 4B). The level remained after 5 days. In all, this indicated production of SDF-1 in CSF of SCI animals.

In vivo bioluminescence imaging (BLI)

After cell transplantation, rats were imaged on day 1, 3, 5, 7, 11, and 14 until sacrifice and cell-derived photons were analyzed using the IVIS 100 (Xenogen) system. Photons could be easily observed in the

transplantation group (Figure 5A). The signals from the site of SCI were quite weak on day 1, almost trapped in the lungs of the rats. It increased on day 3 and gradually became strong in the following days. The increasing signals suggested a growing number of donor cells in the injured spinal cord. On day 11, after injection, total photon emission began to decrease. The signals slowly faded out within 14 days, indicating that most of the donor cells had vanished or died after an initial increase in BLI signal.

For another group, SCI rats were transplanted with MSCs-GFP-Luci after their local injection of SDF-1 (Figure 5B). On day 1, the photon emission increased and was easily detectable compared with the previous group. During the following days, the signals remained strong and maintained at a relatively constant level until they became weak on day 14. The intensity and duration time of cell-provoking signals were stronger and lasted longer than the group without the treatment of SDF-1.

For the third group, MSCs-GFP-Luci were pretreated with AMD3100, the inhibitor of CXCR4 before their injection into SCI rats (Figure 5C). The bioluminescence signal was observed around the whole body, with higher intensity in the lungs on day 1 after injection. High luciferase activity was observed in the spinal cord on day 5 and decreased gradually to the baseline level about two weeks after administration.

Distribution of transplanted MSCs-GFP-Luci in the spinal cord

The anatomical integrity of injured spinal cords in the PBS control group and MSC-transplanted group were evaluated (Figure 6A). Large cavities were found in the spinal cord of rats of the PBS control group. Fewer and smaller cavities were found in the injured spinal cord of rats of the MSC group. Although the tissue structure seemed to be porous, the anatomical integrity of the MSC group was better than that of the PBS group, which suggested that MSCs could promote the tissue regeneration of injured spinal cords.

To examine the dynamic distribution of the transplanted MSCs-GFP-Luci, we observed the fluorescence emission of the sectioned tissues from different groups under the fluorescence microscopy (Figure 6B). On day 1, few GFP-positive cells were detected in the spinal cords in the MSC group, whereas the pretreatment with SDF-1 could increase the number of GFP-positive cells in the spinal cords as compared to MSCs only. By contrast, AM3100 pretreatment led to fewer GFP-positive cells in the spinal cords on day 1. On day 7, more GFP-positive MSCs migrated to the spinal cords as compared to those on day 1. On day 14, the numbers of GFP-positive MSCs were decreased significantly. However, SDF-1 pretreatment could maintain more GFP-positive MSCs in the spinal cords on day 14 as compared to only MSCs. By contrast, AM3100 pretreatment reduced the number of GFP-positive MSCs in the spinal cord on day 14. The results from the GFP fluorescence are similar with those from the above bioluminescence imaging. Taken together, activation of the SDF-1/CXCR4 axis could promote the distribution of MSCs in the injured spinal cords.

Measurement of functional recovery

All groups showed hindlimb dysfunction that was maximal during the first few days after the surgery, with a BBB score of 0 on day 1 after the injury (Figure 6C). MSC-treated animals generally showed better performance of gait than the PBS control animals. In the control group, the BBB score increased to 1.9 on day 7 and to 5.9 on day 28 after injury. In the MSC group, the BBB score increased to 2.5 and 10.5, respectively. From day 7, post-operation, there were significant differences between the MSC-treated animals and the PBS control animals ($P<0.05$). SDF-1-pretreated rats showed a remarkable recovery in locomotion on days 21 and 28, post-operation (BBB scores 11.15 and 11.93). In contrast, rats treated with AMD3100-preincubated MSCs had a BBB score of 6.02 on day 28, showing no significant difference with the PBS control group. These data suggest that activation of SDF-1/CXCR4 axis in MSCs can promote functional recovery in rat models of SCI.

In vitro effect of SDF-1 on CXCR4 expression on MSCs-GFP-Luci

MSCs-GFP-Luci were exposed to SDF-1 for various concentrations (0-400ng/ml) in vitro. The expression of CXCR4 on these cells was determined using PCR analysis. Their expressions remained unchanged during the whole period of incubation (Figure 7A). The negative result suggested that the expression of CXCR4 on MSCs was not affected by SDF-1.

In vitro effect of SDF-1 on the migration of MSCs-GFP-Luci

Transwell migration assay demonstrated the migration of MSCs-GFP-Luci in response to various concentrations (0-400 ng/ml) of SDF-1. SDF-1 induced MSCs-GFP-Luci migration in a dose-dependent manner, with the maximum observed at 200 ng/ml of SDF-1 (Figure 7B). This result indicated the relevance of SDF-1/CXCR4 axis in the migration of MSCs. The number of migrated MSCs-GFP-Luci to SDF-1 was decreased when the effective concentrations of SDF-1 were added into both the top and bottom chambers in the assays (data not shown).

In vitro effect of AMD3100 on the migration of MSCs-GFP-Luci in response to SDF-1

MSCs were pretreated with AMD3100 before the migration assay. The pretreatment of MSCs with AMD3100 abrogated the effect of SDF-1 at its optimal concentration (Figure 7C). Therefore, the in vitro data might indicate that CXCR4 plays a role in the engraftment of these cells in the spinal cord of SCI rats.

Effect of CSF collected from SCI rats on the migration of MSCs-GFP-Luci

To investigate the capacity of CSF to induce the migration of MSCs-GFP-Luci, we collected four concentrations of CSF (5, 10, 20, and 30%) from rats at 5 days after SCI and normal rats and tested their effects by using the in vitro migration model (Figure 8A). The chemotactic effect of CSF on MSCs-GFP-Luci was dose-dependent at concentrations of 5-20%. The significant chemotactic activity was observed at 20% of CSF. However, with a higher concentration, the number of migrated MSCs-GFP-Luci decreased instead. It might be caused by the increasing number of dead cells with a higher concentration of CSF.

MSCs-GFP-Luci were pretreated with AMD3100 or SDF-1 antibody for 30 min before the migration assay. Both AMD3100 and SDF-1 antibody significantly decreased CSF-induced migration (Figure 8B). This study indicated that the SDF-1/CXCR4 reaction is a main but not the only chemotactic mechanism in regulating the migration of MSCs.

Discussion

Severe SCI usually results in long-lasting deficits involving partial or complete paralysis and loss of sensation below the level of the injury [22]. Because intrinsic repair is limited after SCI, the development of new strategies to treat such injuries is a major clinical challenge. Nowadays, a variety of experimental strategies, including stem cell transplantation, are emerging to promote regeneration of the injured spinal cord [22–24]. The primary objectives of such cellular transplants are to enhance neuronal survival and create permissive conditions for the regeneration of injured tissue. The identification of a rich source of appropriate cells for replacement or inductive therapies is one of the most important steps in this process. Among the different stem cell sources available, MSC is an abundant source of immature immune cells, with no ethical concerns [14, 25]. They can be easily acquired, maintained, expanded quickly, and differentiated into neural cell types in vitro and in vivo [26, 27]. No invasive procedures are required to obtain bone marrow-derived MSCs, and it has been safely used clinically. Furthermore, MSCs were reported to have an ability to home to tissues, particularly when injured or inflamed, involving migration across endothelial cell layers [3, 28]. Thus, these attractive features encourage the investigation of bone marrow-derived MSCs as therapeutic tools and are leading us to potential uses for cell therapy of SCI.

While the migratory behavior of MSCs has now been extensively reported [29], we have yet to determine what signal guides migration of MSCs to specific in vivo targets. If such a signal exists, what molecule mediates the migration of MSCs? Inflammation at wound sites appears to be an initial signal, in which the homing and migration of leukocytes are promoted for the first defense through the deployment of chemokines and receptors [30]. It has recently been shown that MSCs also express some of these molecules. Hence, it is likely that injured tissue expresses specific ligands to facilitate trafficking, adhesion, and infiltration of MSCs to the site of injury, as is the case with the recruitment of leukocytes to sites of inflammation [31]. Among these components, SDF-1 and its receptor CXCR4 are crucial for bone marrow retention, mobilization, and are involved in homing and recruitment of stem cells to sites of injured tissues [17]. SDF-1 has been reported to be expressed in a wide range of issues, including those of the heart, skeleton, live, pancreas, endothelium, skin, and spinal cord [20, 32–36]. Recent studies suggest

that the interaction of SDF-1 and CXCR4 could partially mediate the trafficking of MSCs to the impaired nucleus in the brain [20, 37]. Here, we examined the role of the SDF-1/CXCR4 axis in the migration of MSCs to the site of the injured spinal cord.

Recent studies confirm the potential therapeutic application of bone marrow-derived MSCs in animal models of neurological disease, including SCI, stroke, and sclerosis [38–40]. The rat is the animal most frequently used in models of SCI, because of low cost, size, and accessibility. Given the fact that similar neurological injuries may occur in most cases of SCI, we have developed a standard contusion injury model of rat, in which the spinal cord is vertically contused from a defined height and with a fixed force correlating with severe neurological injury and weak functional recovery. In previous studies, cell transplantation for SCI was performed by direct injection into the injured spinal cord parenchyma [41–43]. However, direct injection into the spine lesion with a needle would be clinically unrealistic, and the procedure itself is potentially harmful to the parenchyma. Less invasive techniques suited for the clinical application need to be developed. Trials by intravenous injections of MSCs in rodents were widely reported [44–48]. Cultured rat and human MSCs have been shown to migrate into sites of brain injury after cerebral ischemia when transplanted intravenously in rats [49]. MSCs have also been used to treat lung injury in mice when administered by the intravenous route [50]. In clinical trials, cultured MSCs have been administered systemically to humans to treat several conditions, including osteogenesis imperfecta (OI) [51]. Hence, the systemic delivery of manipulated MSCs indeed provides a feasible therapeutic approach for cell therapy in SCI.

No previously reported study has tracked MSCs that were intravenously transplanted into the spinal cord in living animals; to date, only histological assessments have confirmed the fate of stem cells after their systemic transplantation [27, 44–48]. These studies did not evaluate the survival, proliferation, and migration of transplanted cells. Given this, we used the cell tracing technique to achieve repeated and non-invasive monitoring of the fate of transplanted cells and clarify the factors needed for successful engraftment of donor cells and assessing the safety of their transplantation. In this study, we harvested MSCs from GFP-transgenic rats and transfected them with luciferase and then focused on the characteristic migration of MSCs-GFP-Luci to injury sites. The repetitive in vivo bioimaging of luciferase activity could continually monitor the cell distribution, noninvasively, in individual animals in a simple and rapid fashion [52], and provided us with a better perspective on the behavior of transplanted cells.

We systemically transplanted GFP- and luciferase-expressing MSCs into rats subjected to spinal cord contusion. We first observed the increased expression of SDF-1 in the injured spinal cord, indicating the involvement of SDF-1 in the acute phase of SCI. Moreover, the increased temporal expression of SDF-1 paralleled the number of migrated MSCs (Fig. 2 and Fig. 5A). However, when CXCR4 on MSCs was blocked with AMD3100, we still detected the expression of CXCR4 in the injured site (Fig. 3C), indicating that there may be some other chemokines involving in MSC migration, or that some endogenous cells expressing CXCR4 migrated to the injury site. The in vivo BLI showed that transplanted MSCs-GFP-Luci migrated toward the injury site after they were getting trapped in the lungs for a short time (Fig. 5A). The number of migrated donor cells significantly increased when SCI rats were pretreated with SDF-1

(Fig. 5B). In contrast, the pretreatment with the CXCR4-specific antagonist AMD3100 markedly prevented the migration of MSCs to the lesion site (Fig. 5C). The findings were verified by histological evaluation (Fig. 6). On histological analysis, the transplanted MSCs-GFP-Luci were distributed surrounding the impaired site. Because the model of spinal cord contusion used in this study produces a cavity of injury, the transplanted MSCs-GFP-Luci most likely distributed around the site of injury and were unable to pass over it. All in vivo results suggested that MSCs-GFP-Luci did have the ability to migrate to the injured spinal cord in response to SDF-1 expressed by damaged tissue. The CSF level of SDF-1 was also found to be increased, but not significantly (Fig. 4). We speculated that a small amount of SDF-1 secreted from the injured spinal cord flowed to the CSF through the incomplete open central canal caused by the injury. So, we collected the CSF from the SCI rats to induce MSC migration in vitro to simulate the migration of MSCs in vivo.

In vitro study showed that the expression of CXCR4 on MSCs. The expression level remained unchanged when MSCs were incubated with SDF-1 (Fig. 7A), suggesting that the expression of CXCR4 on MSCs-GFP-Luci was not affected by SDF-1. Transwell migration assay demonstrated that SDF-1 induced MSCs-GFP-Luci migration in a dose-dependent manner, while the pretreatment of MSCs-GFP-Luci with AMD3100 abrogated the effect of SDF-1 (Fig. 7B and 7C), indicating the relevance of SDF-1/CXCR4 in MSC migration. Moreover, the chemotactic effect of CSF collected from SCI rats on MSCs-GFP-Luci was also dose-dependent at a certain concentration range (Fig. 8). With a higher concentration of CSF in the medium (> 20%), the environment required for cell survival changed considerably, causing more cells to die (Fig. 8A). After MSCs-GFP-Luci were pretreated with AMD3100 or SDF-1 antibody, CSF induced migration was significantly abrogated, but not completely blocked (Fig. 8B). This result indicated that the SDF-1/CXCR4 reaction is a main but not the only chemotactic mechanism in regulating the engraftment of MSCs in the spinal cord of SCI rats.

It is known that the adult CNS, especially the injured CNS, may provide a relatively non-permissive environment for transplanted MSCs and other stem cells [43, 53, 54]. Even under the best circumstances, cell survival in injured CNS has been estimated to be less than 10% [43, 55, 56]. In our study, therefore, with increasing time post-transplantation, the number of transplanted MSCs-GFP-Luci gradually decreased, and few could survive on d 14 (Fig. 5). One of the most important reasons why those cells could not survive in the injured spinal cord for a long time is probably due to the sustained inflammation in the injury sites or the immediate inflammatory response elicited by surgery and injection manipulation [53, 56, 57].

Our results further indicated that systemic delivery of MSCs-GFP-Luci could stimulate tissue regeneration, reduce lesion size, and promote the functional recovery from SCI, as determined by histological analysis and improved behavioral outcome. The anatomical integrity of the injured spinal cord was better in MSC-treated rats than in PBS-treated ones. The rats received MSCs also displayed a more rapid recovery of BBB assessment performance than the control rats receiving PBS only. Our interpretation of these data is that the transplanted MSCs reach the site of injury and provide a neuroprotective effect for endogenous tissue repair and regeneration. The mechanisms underlying the beneficial effect need to be defined. First,

transdifferentiation of MSC into neurons and myelin-forming cells may occur in the regenerated tissue after they reach the injury site. However, the time for which the transplanted MSCs could survive is relatively short, not sufficient for these donor cells to be induced to transdifferentiate into functional cells and further contribute to the endogenous neural repair. Second, the intrinsic secretory activity of MSCs also establishes a regenerative microenvironment at sites of tissue injury or damage. These bioactive factors are supposed to limit the area of damage and to mount a self-regulated regenerative response. They may inhibit scarring, inhibit apoptosis, stimulate angiogenesis, and stimulate the mitosis of tissue-intrinsic stem or progenitor cells. This complex, multifaceted activity caused by the secretory activity of MSCs is referred to as trophic activity, as distinctive from the capacity of MSCs to differentiate.

Conclusions

Different cellular transplantation strategies have shown some efficacy in treating SCI, although very few have been translated into clinical trials. Before clinical application, it is necessary to generate sufficient preclinical data regarding the efficacy and the biological mechanisms of any functional improvement. Results from this study suggest that intravenous delivery of bone marrow-derived MSCs results in their specific migration to the injury site of the spinal cord and that the interaction of SDF-1 and CXCR4 is involved in MSC migration. Harnessing the migratory potential of MSCs by modulating their chemokine-chemokine receptor interaction may be a powerful way to enhance the recruitment of ex vivo-cultured MSCs and increase their therapeutic potential in the damaged or diseased tissues. However, further investigation may be necessary to determine the specific roles of the exogenous MSCs and make clear how these donor cells participate in the injury response and contribute to the neuroprotection in the injured spinal cord.

Abbreviations

SCI: spinal cord injury; MSC: mesenchymal stem cell; SDF-1: stromal cell-derived factor 1; CXCR4: C-X-C chemokine receptor type 4; CSF: Cerebrospinal fluid.

Declarations

Acknowledgments

Not applicable.

Authors’ contributions

SC designed and executed most of the experiments, coordinated the collaborations, data analyses and manuscript writing. YY executed part of experiments. ADZ and XHP completed the data analysis and manuscript writing. YP reviewed and edited the manuscript. All authors approved the final manuscript.

Funding

This work was supported by National Natural Science Foundation of China (No. 81272080, 81000011, and 81000835); by Science and Technology Planning Project of Shenzhen Municipality (No. JCYJ20180305123654620, JCYJ20120613101917373 and JC201005280429A); by Natural Science Foundation of Guangdong Province (No. 2016A030313797).

Availability of data and materials

The data supporting the conclusions of this article are included within the article.

Ethics approval and consent to participate

All animal experiments were performed with permission from the Institutional Animal

Care and Use Committees of Shenzhen University.

Consent for publication

Not applicable.

Competing interests

The authors declare that they have no competing interests.

Author details

[1] Health Science Center, Shenzhen University, Shenzhen, China

[2] Department of Trauma and Orthopedics, The 2nd Affiliated Hospital of Shenzhen University, The Affiliated Baoan Hospital of Southern Medical University, Shenzhen, China

References

1. Uccelli A, Moretta L, Pistoia V. Mesenchymal stem cells in health and disease. Nat Rev Immunol. 2008;8:726–36.
2. Wang Y, Chen X, Cao W, Shi Y. Plasticity of mesenchymal stem cells in immunomodulation: pathological and therapeutic implications. Nat Immunol. 2014;15:1009–16.

3. Nombela-Arrieta C, Ritz J, Silberstein LE. The elusive nature and function of mesenchymal stem cells. Nat Rev Mol Cell Biol. 2011;12:126–31.
4. Barry F, Murphy M. Mesenchymal stem cells in joint disease and repair. Nat Rev Rheumatol. 2013;9:584–94.
5. Herrmann M, Verrier S, Alini M. Strategies to Stimulate Mobilization and Homing of Endogenous Stem and Progenitor Cells for Bone Tissue Repair. Front Bioeng Biotechnol. 2015;3:79.
6. Lee CW, Chen YF, Wu HH, Lee OK. Historical Perspectives and Advances in Mesenchymal Stem Cell Research for the Treatment of Liver Diseases. Gastroenterology. 2018;154:46–56.
7. Walter J, Ware LB, Matthay MA. Mesenchymal stem cells: mechanisms of potential therapeutic benefit in ARDS and sepsis. The Lancet Respiratory Medicine. 2014;2:1016–26.
8. Matsushita K. Heart Failure and Adipose Mesenchymal Stem Cells. Trends Mol Med. 2020;26:369–79.
9. Cai S, Shea GK, Tsui AYP, Chan YS, Shum DKY. Derivation of clinically applicable schwann cells from bone marrow stromal cells for neural repair and regeneration. CNS Neurol Disord Drug Targets. 2011;10:500–8.
10. Pan Y, Cai S. Current state of the development of mesenchymal stem cells into clinically applicable Schwann cell transplants. Mol Cell Biochem. 2012;368:127–35.
11. Cai S, Tsui YP, Tam KW, Shea GKH, Chang RSK, Ao Q, et al. Directed Differentiation of Human Bone Marrow Stromal Cells to Fate-Committed Schwann Cells. Stem Cell Reports. 2017;9:1097–108.
12. Cai S, Han L, Ao Q, Chan YS, Shum DKY. Human Induced Pluripotent Cell-Derived Sensory Neurons for Fate Commitment of Bone Marrow-Derived Schwann Cells: Implications for Remyelination Therapy: Implications for Remyelination Therapy. Stem Cells Transl Med. 2017;6:369–81.
13. Cai S, Pan Y, Han B, Sun TZ, Sheng ZY, Fu XB. Transplantation of human bone marrow-derived mesenchymal stem cells transfected with ectodysplasin for regeneration of sweat glands. Chin Med J. 2011;124:2260–8.
14. Ankrum JA, Ong JF, Karp JM. Mesenchymal stem cells: immune evasive, not immune privileged. Nat Biotechnol. 2014;32:252–60.
15. Lau TT, Wang DA. Stromal cell-derived factor-1 (SDF-1): homing factor for engineered regenerative medicine. Expert Opin Biol Ther. 2011;11:189–97.
16. Chavakis E, Urbich C, Dimmeler S. Homing and engraftment of progenitor cells: a prerequisite for cell therapy. J Mol Cell Cardiol. 2008;45:514–22.
17. Nagasawa T. CXCL12/SDF-1 and CXCR4. Front Immunol. 2015;6:301.
18. Cheng X, Wang H, Zhang X, Zhao S, Zhou Z, Mu X, et al. The Role of SDF-1/CXCR4/CXCR7 in Neuronal Regeneration after Cerebral Ischemia. Front Neurosci. 2017;11:590.
19. Wang Y, Deng Y, Zhou GQ. SDF-1alpha/CXCR4-mediated migration of systemically transplanted bone marrow stromal cells towards ischemic brain lesion in a rat model. Brain Res. 2008;1195:104–12.

20. Deng QJ, Xu XF, Ren J. Effects of SDF-1/CXCR4 on the Repair of Traumatic Brain Injury in Rats by Mediating Bone Marrow Derived Mesenchymal Stem Cells. Cell Mol Neurobiol. 2018;38:467–77.
21. Matyas JJ, Stewart AN, Goldsmith A, Nan Z, Skeel RL, Rossignol J, Dunbar GL. Effects of Bone-Marrow-Derived MSC Transplantation on Functional Recovery in a Rat Model of Spinal Cord Injury: Comparisons of Transplant Locations and Cell Concentrations. Cell Transplant. 2017;26:1472–82.
22. Gong Z, Xia K, Xu A, Yu C, Wang C, Zhu J, et al. Stem cell transplantation: A promising therapy for spinal cord injury. Curr Stem Cell Res Ther. 2019;15:321–31.
23. Deng W-S, Ma K, Liang B, Liu X-Y, Xu H-Y, Zhang J, et al. Collagen scaffold combined with human umbilical cord-mesenchymal stem cells transplantation for acute complete spinal cord injury. Neural Regen Res. 2020;15:1686–700.
24. Jin MC, Medress ZA, Azad TD, Doulames VM, Veeravagu A. Stem cell therapies for acute spinal cord injury in humans: a review. Neurosurg Focus. 2019;46:E10.
25. Gebler A, Zabel O, Seliger B. The immunomodulatory capacity of mesenchymal stem cells. Trends Mol Med. 2012;18:128–34.
26. Zhan J, Li X, Luo D, Hou Y, Hou Y, Chen S, et al. Polydatin promotes the neuronal differentiation of bone marrow mesenchymal stem cells in vitro and in vivo: Involvement of Nrf2 signalling pathway. J Cell Mol Med. 2020;24:5317–29.
27. Zhang XM, Ma J, Sun Y, Yu BQ, Jiao ZM, Wang D, et al. Tanshinone IIA promotes the differentiation of bone marrow mesenchymal stem cells into neuronal-like cells in a spinal cord injury model. J Transl Med. 2018;16:193.
28. Karp JM, Leng Teo GS. Mesenchymal stem cell homing: the devil is in the details. Cell Stem Cell. 2009;4:206–16.
29. Fu X, Liu G, Halim A, Ju Y, Luo Q, Song AG. Mesenchymal Stem Cell Migration and Tissue Repair. Cells. 2019;8:784.
30. Powell D, Tauzin S, Hind LE, Deng Q, Beebe DJ, Huttenlocher A. Chemokine Signaling and the Regulation of Bidirectional Leukocyte Migration in Interstitial Tissues. Cell Rep. 2017;19:1572–85.
31. Zachar L, Bačenková D, Rosocha J. Activation, homing, and role of the mesenchymal stem cells in the inflammatory environment. J Inflamm Res. 2016;9:231–40.
32. Penn MS, Pastore J, Miller T, Aras R. SDF-1 in myocardial repair. Gene Ther. 2012;19:583–7.
33. Qin HJ, Xu T, Wu HT, Yao ZL, Hou YL, Xie YH, et al. SDF-1/CXCR4 axis coordinates crosstalk between subchondral bone and articular cartilage in osteoarthritis pathogenesis. Bone. 2019;125:140–50.
34. Jaerve A, Bosse F, Müller HW. SDF-1/CXCL12: its role in spinal cord injury. Int J Biochem Cell Biol. 2012;44:452–6.
35. Li G, An J, Han X, Zhang X, Wang W, Wang S. Hypermethylation of microRNA-149 activates SDF-1/CXCR4 to promote osteogenic differentiation of mesenchymal stem cells. J Cell Physiol. 2019;234:23485–94.

36. Gong J, Meng HB, Hua J, Song ZS, He ZG, Zhou B, Qian MP. The SDF-1/CXCR4 axis regulates migration of transplanted bone marrow mesenchymal stem cells towards the pancreas in rats with acute pancreatitis. Mol Med Rep. 2014;9:1575–82.
37. Wang Y, Fu W, Zhang S, He X, Liu Z, Gao D, Xu T. CXCR-7 receptor promotes SDF-1α-induced migration of bone marrow mesenchymal stem cells in the transient cerebral ischemia/reperfusion rat hippocampus. Brain Res. 2014;1575:78–86.
38. Oh K-W, Noh M-Y, Kwon M-S, Kim HY, Oh S-I, Park J, et al. Repeated Intrathecal Mesenchymal Stem Cells for Amyotrophic Lateral Sclerosis. Ann Neurol. 2018;84:361–73.
39. Lim S, Yoon HY, Jang HJ, Song S, Kim W, Park J, et al. Dual-Modal Imaging-Guided Precise Tracking of Bioorthogonally Labeled Mesenchymal Stem Cells in Mouse Brain Stroke. ACS Nano. 2019;13:10991–1007.
40. Ning GZ, Song WY, Xu H, Zhu RS, Wu QL, Wu Y, et al. Bone marrow mesenchymal stem cells stimulated with low-intensity pulsed ultrasound: Better choice of transplantation treatment for spinal cord injury: Treatment for SCI by LIPUS-BMSCs transplantation. CNS Neurosci Ther. 2019;25:496–508.
41. Sun L, Wang F, Chen H, Liu D, Qu T, Li X, et al. Co-Transplantation of Human Umbilical Cord Mesenchymal Stem Cells and Human Neural Stem Cells Improves the Outcome in Rats with Spinal Cord Injury. Cell Transplant. 2019;28:893–906.
42. Chudickova M, Vackova I, Machova Urdzikova L, Jancova P, Kekulova K, Rehorova M, et al. The Effect of Wharton Jelly-Derived Mesenchymal Stromal Cells and Their Conditioned Media in the Treatment of a Rat Spinal Cord Injury. Int J Mol Sci. 2019;20:4516.
43. Allahdadi KJ, Santana TA de, Santos GC, Azevedo CM, Mota RA, Nonaka CK, et al. IGF-1 overexpression improves mesenchymal stem cell survival and promotes neurological recovery after spinal cord injury. Stem Cell Res Ther. 2019;10:146.
44. Chen L, Cui X, Wu Z, Jia L, Yu Y, Zhou Q, et al. Transplantation of bone marrow mesenchymal stem cells pretreated with valproic acid in rats with an acute spinal cord injury. Biosci Trends. 2014;8:111–9.
45. Yang C, Wang G, Ma F, Yu B, Chen F, Yang J, et al. Repeated injections of human umbilical cord blood-derived mesenchymal stem cells significantly promotes functional recovery in rabbits with spinal cord injury of two noncontinuous segments. Stem Cell Res Ther. 2018;9:136.
46. Vawda R, Badner A, Hong J, Mikhail M, Lakhani A, Dragas R, et al. Early Intravenous Infusion of Mesenchymal Stromal Cells Exerts a Tissue Source Age-Dependent Beneficial Effect on Neurovascular Integrity and Neurobehavioral Recovery After Traumatic Cervical Spinal Cord Injury. Stem Cells Transl Med. 2019;8:639–49.
47. Oshigiri T, Sasaki T, Sasaki M, Kataoka-Sasaki Y, Nakazaki M, Oka S, et al. Intravenous Infusion of Mesenchymal Stem Cells Alters Motor Cortex Gene Expression in a Rat Model of Acute Spinal Cord Injury. J Neurotrauma. 2019;36:411–20.

48. Morita T, Sasaki M, Kataoka-Sasaki Y, Nakazaki M, Nagahama H, Oka S, et al. Intravenous infusion of mesenchymal stem cells promotes functional recovery in a model of chronic spinal cord injury. Neuroscience. 2016;335:221–31.
49. Honmou O, Onodera R, Sasaki M, Waxman SG, Kocsis JD. Mesenchymal stem cells: therapeutic outlook for stroke. Trends Mol Med. 2012;18:292–7.
50. Liu D, Kong F, Yuan Y, Seth P, Xu W, Wang H, et al. Decorin-Modified Umbilical Cord Mesenchymal Stem Cells (MSCs) Attenuate Radiation-Induced Lung Injuries via Regulating Inflammation, Fibrotic Factors, and Immune Responses. Int J Radiat Oncol Biol Phys. 2018;101:945–56.
51. Götherström C, Westgren M, Shaw SWS, Aström E, Biswas A, Byers PH, et al. Pre- and postnatal transplantation of fetal mesenchymal stem cells in osteogenesis imperfecta: a two-center experience. Stem Cells Transl Med. 2014;3:255–64.
52. Yan Y, Shi P, Song W, Bi S. Chemiluminescence and Bioluminescence Imaging for Biosensing and Therapy: In Vitro and In Vivo Perspectives. Theranostics. 2019;9:4047–65.
53. Hakim R, Covacu R, Zachariadis V, Frostell A, Sankavaram SR, Brundin L, Svensson M. Mesenchymal stem cells transplanted into spinal cord injury adopt immune cell-like characteristics. Stem Cell Res Ther. 2019;10:115.
54. Torres-Espín A, Redondo-Castro E, Hernandez J, Navarro X. Immunosuppression of allogenic mesenchymal stem cells transplantation after spinal cord injury improves graft survival and beneficial outcomes. J Neurotrauma. 2015;32:367–80.
55. Wang W, Huang X, Lin W, Qiu Y, He Y, Yu J, et al. Hypoxic preconditioned bone mesenchymal stem cells ameliorate spinal cord injury in rats via improved survival and migration. Int J Mol Med. 2018;42:2538–50.
56. Mukhamedshina Y, Gracheva O, Mukhutdinova D, Chelyshev Y, Rizvanov A. Mesenchymal stem cells and the neuronal microenvironment in the area of spinal cord injury. Neural Regen Res. 2019;14:227.
57. Khan IU, Yoon Y, Kim A, Jo KR, Choi KU, Jung T, et al. Improved Healing after the Co-Transplantation of HO-1 and BDNF Overexpressed Mesenchymal Stem Cells in the Subacute Spinal Cord Injury of Dogs. Cell Transplant. 2018;27:1140–53.

Figures

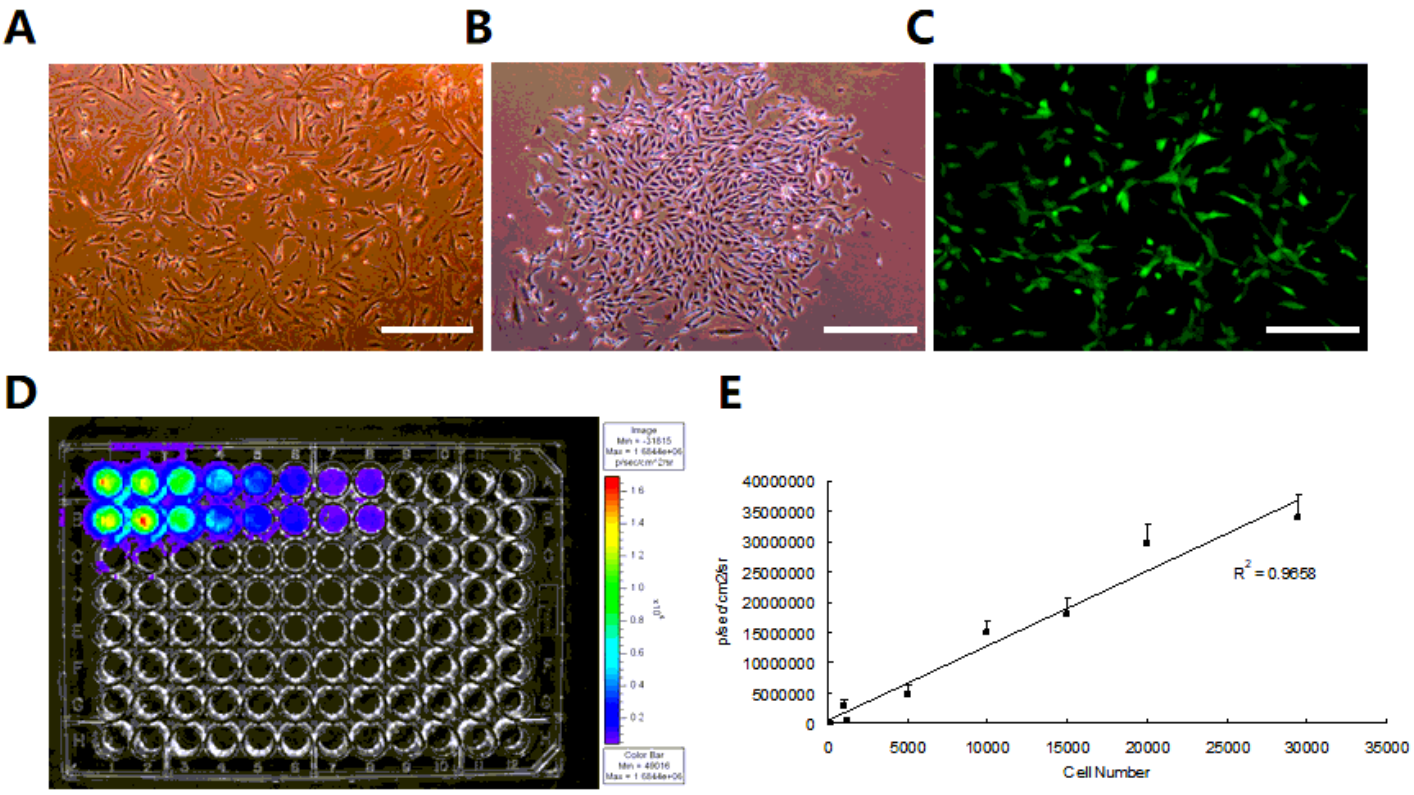

Figure 1

Characteristics of rat bone marrow-derived MSCs-GFP-Luci. (A) MSCs-GFP-Luci showed a fibroblast-like morphology (original magnification ×200) under a microscope. (B) MSCs-GFP-Luci formed colonies with fine edges (original magnification ×200). (C) MSCs-GFP-Luci isolated from GFP transgenic rats expressed GFP (original magnification ×200). (D) MSCs-GFP-Luci were incubated with luciferin, and photon emission was measured with the Xenogen IVIS system. Bioluminescence imaging (BLI) signal from luciferase expression reflects viable cell numbers. BLI of varying numbers of cells (100, 500, 1000, 5000, 10000, 15000, 20000, and 30000) in a 96-well plate showed a correlation with increasing signals. (E) Regression analysis revealed a significant linear increase of luminescence with cell numbers. Scale bars=100 μm (A-C).

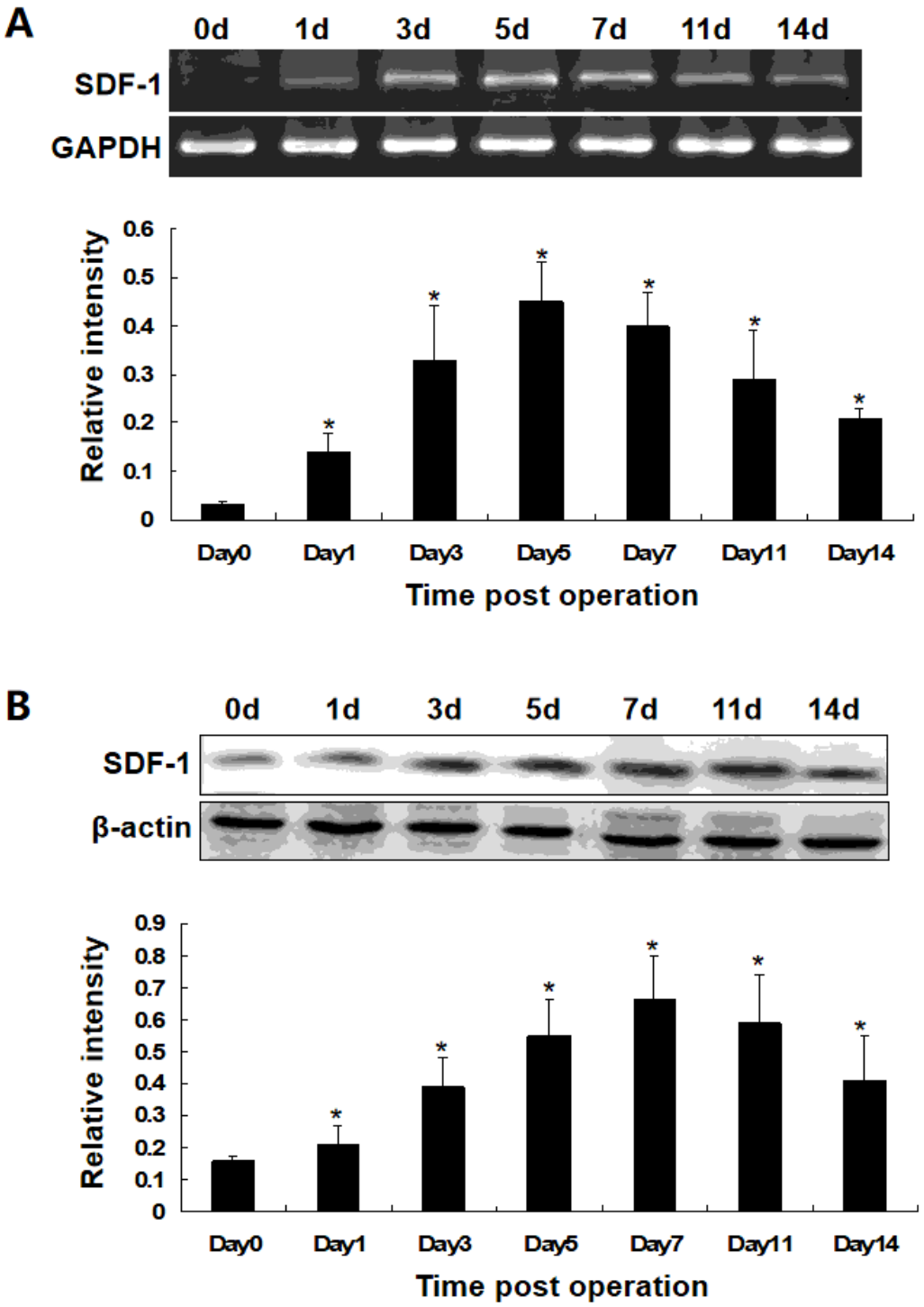

Figure 2

Expression of SDF-1 in the injured spinal cords. (A) Expression of SDF-1 mRNA in the injured spinal cords. (B) Expression of SDF-1 protein in the injured spinal cords. The relative intensity was determined by the ratio of the specific marker to GAPDH or β-actin, as measured by densitometry. Results are representative of 3 independent experiments. Bar with * is significantly different ($P<0.05$).

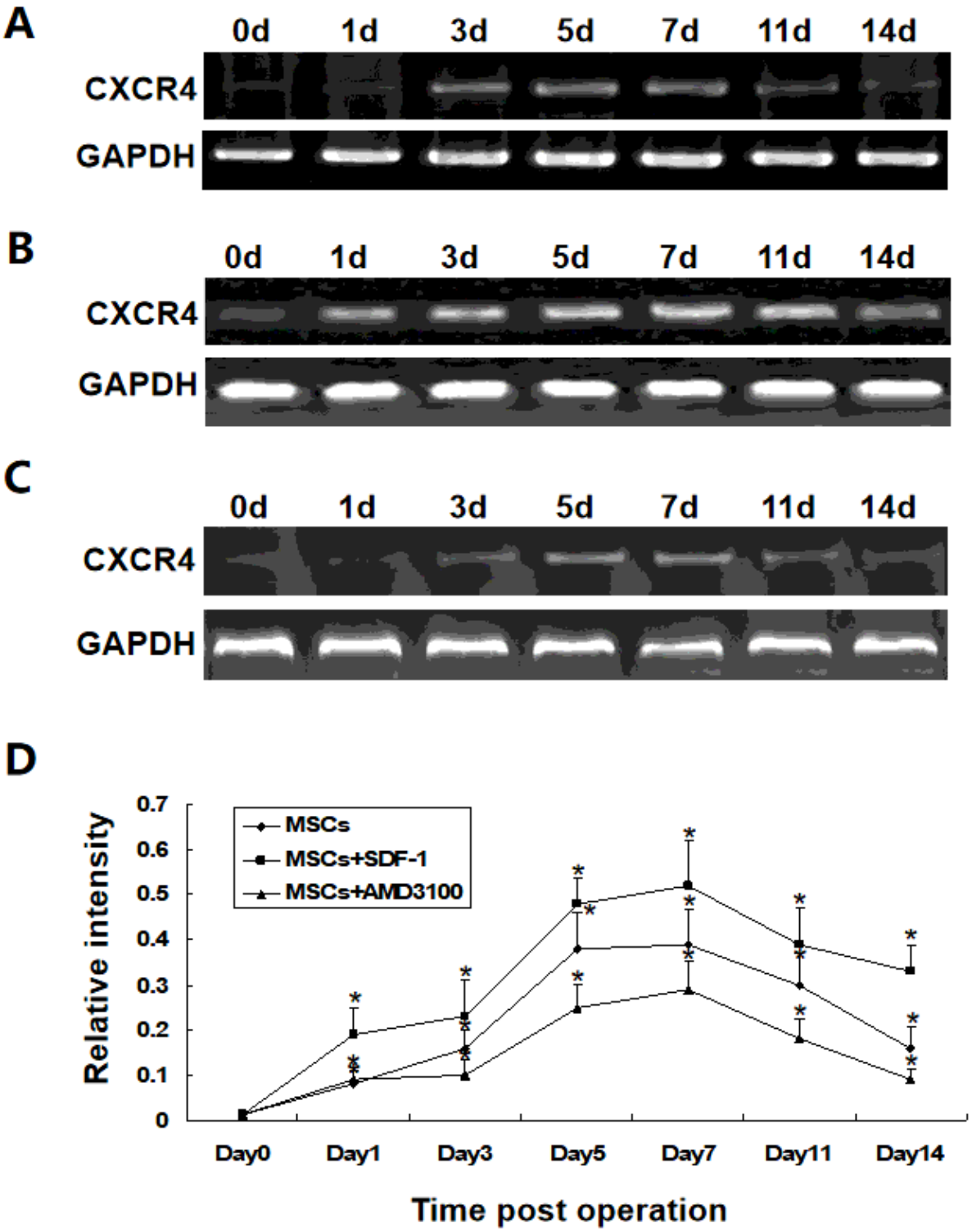

Figure 3

Expression of CXCR4 in the injured spinal cords. (A) Expression of CXCR4 mRNA in spinal cords after transplantation of MSCs-GFP-Luci. (B) Expression of CXCR4 mRNA in spinal cords after the pretreatment of SDF-1 and transplantation of MSCs-GFP-Luci. (C) Expression of CXCR4 mRNA in spinal cords after transplantation of AMD3100-preincubated MSCs-GFP-Luci. (D) The relative intensity was determined by

the ratio of the specific marker to GAPDH as measured by densitometry. Results are representative of 3 independent experiments. Bar with * is significantly different (P<0.05).

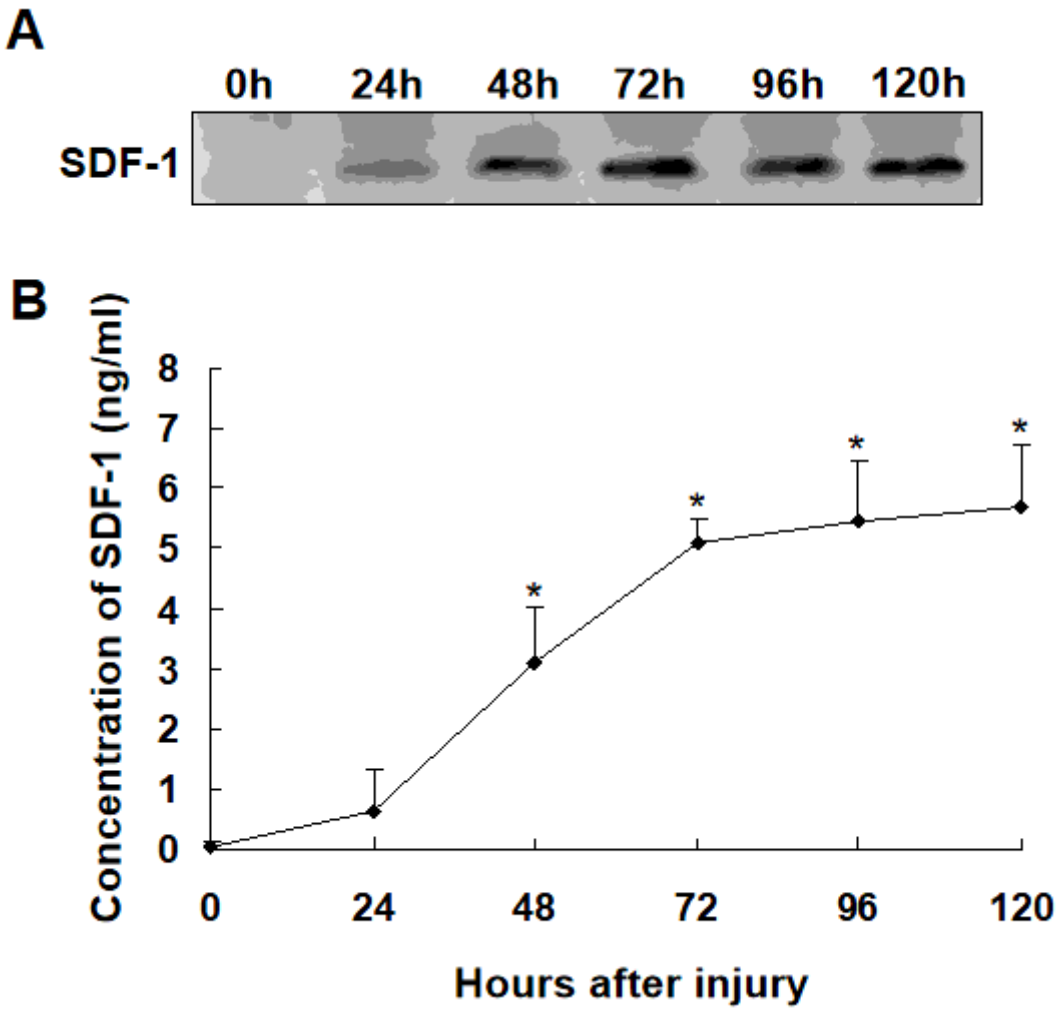

Figure 4

SDF-1 level in the CSF of SCI rats. SDF-1 was detected in CSF at different time points of before and 24, 48, 72, 96, and 120 hours after SCI by western blotting analysis (A) and ELISA (B). Data are presented as mean±SD. Bar with * is significantly different (P<0.05).

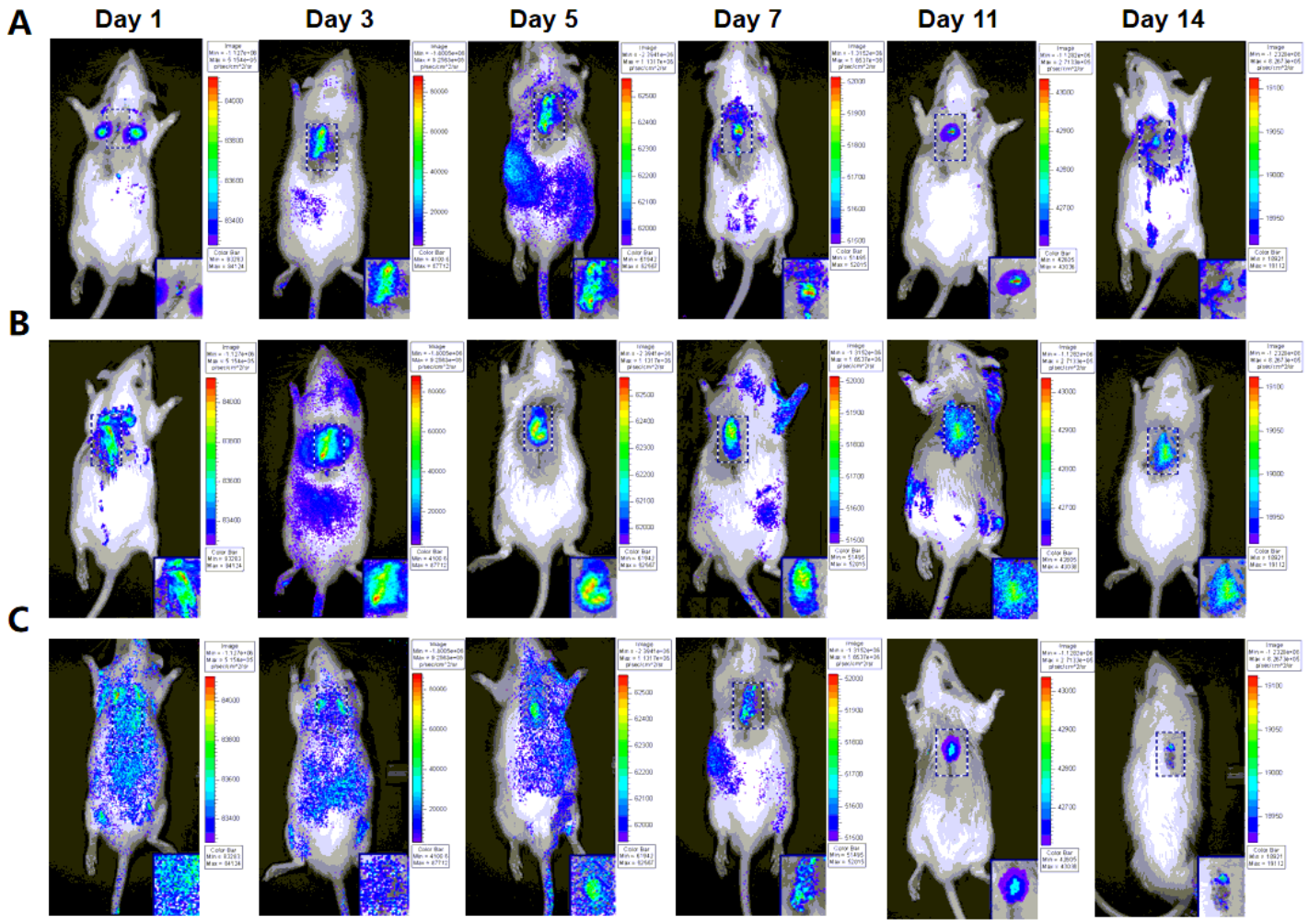

Figure 5

In vivo distribution of intravenously administered MSC-GFP-Luci. Representative bioluminescent images showed MSCs-GFP-Luci location after intravenous administration at 1, 3, 5, 7, 11, and 14 days. (A) Intravenous injection of MSCs-GFP-Luci in SCI rats. BLI showed the accumulation of MSCs in the lungs on day 1 after injection. On day 3, MSCs homed in the spinal cord. The increasing signals suggested a growing number of cells in the injured spinal cord. After day 11, the decreasing signal intensity is indicative of acute donor cell death. (B) Intravenous injection of MSCs-GFP-Luci in SCI rats after injection of SDF-1. On day 1, BLI showed retention of transplanted cells not only in the lung but also in the spinal cord. BLI signals over the spinal cord revealed an increase in signal from day 1 to day 7 and maintained a constant level on day 11. It gradually became weak on day 14. (C) Intravenous injection of MSCs-GFP-Luci pretreated with AMD3100. The bioluminescence signal was observed around the whole body, with higher intensity in the lungs on day 1 after injection. High luciferase activity was observed in the spinal cord on day 5 and decreased gradually to the baseline level about two weeks after administration.

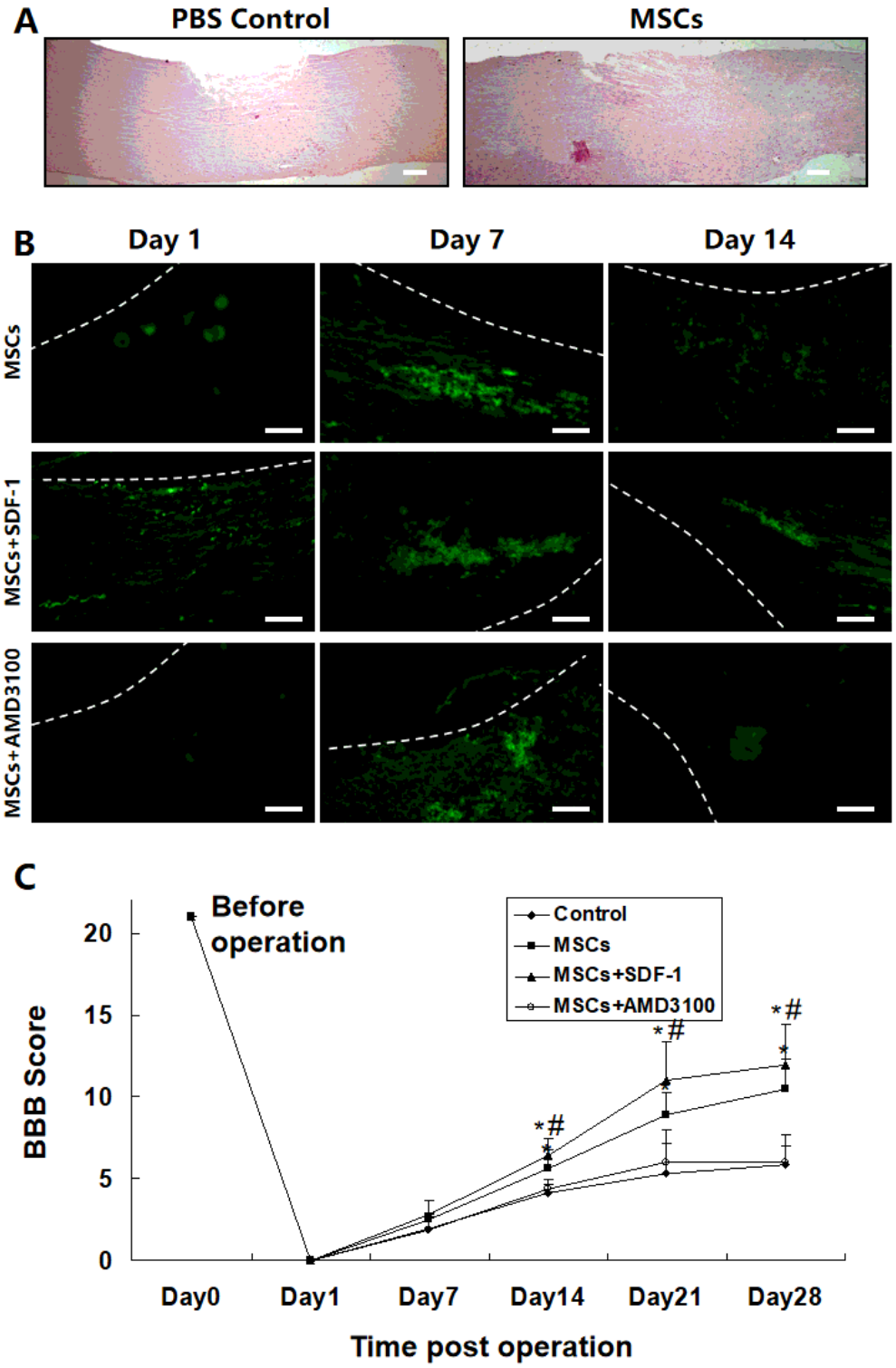

Figure 6

Distribution of transplanted MSCs-GFP-Luci and time course of locomotor recovery evaluated by BBB scores (n=6). (A) Hematoxylin-eosin (HE) analysis of the histological tissues of the injured spinal cords from control mice treated with PBS and mice treated with MSCs-GFP-Luci. (B) Immunohistochemistry analysis of the distribution of MSCs-GFP-Luci in the injured spinal cords in different groups on day 1, 7, and 14 after transplantation. MSCs group: mice received an intravenous injection of MSCs-GFP-Luci only;

MSCs+SDF-1 group: mice received an intravenous injection of MSCs-GFP-Luci and pretreatment with SDF-1; MSCs+AMD3100: mice received an intravenous injection of MSCs-GFP-Luci that were pretreated with AMD3100. Scale bars=100 μm (A and B). (C) Performance in locomotor function was enhanced in the MSC-treated animals compared with the PBS control animals. A statistical difference in the BBB scores was achieved 1 week after transplantation. After 3 weeks, there was a significant difference on the BBB scale between the MSC and PBS groups. After pretreatment with SDF-1, animals treated with MSCs had more improved motor function than the animals transplanted with MSCs only. However, the animals treated with AMD3100-preincubated MSCs had lower BBB scores than the MSC-treated animals. Data are presented as mean±SD, *P<0.05 vs control, #P<0.05 vs MSC.

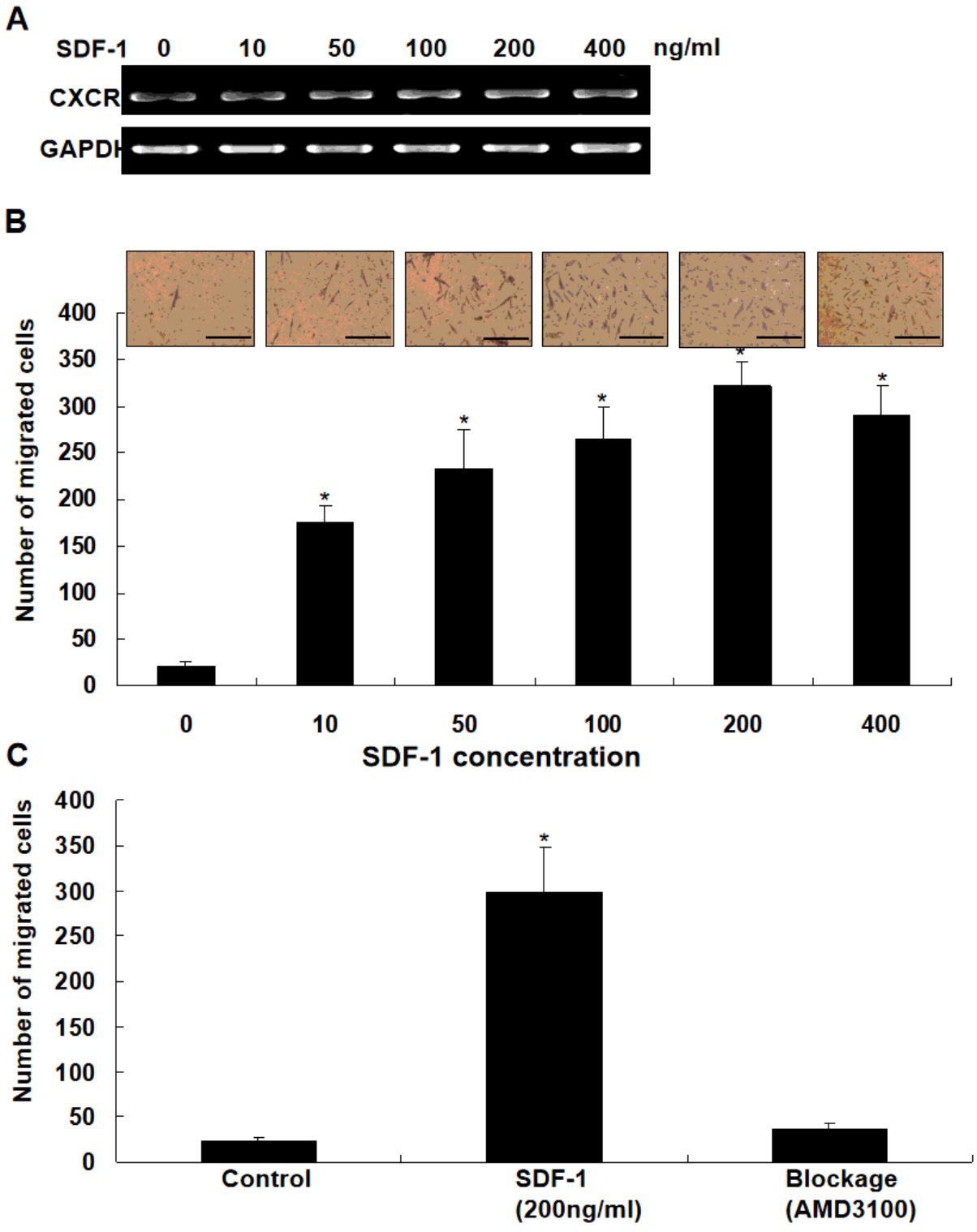

Figure 7

Effect of SDF-1 on the expression of CXCR4 on and migration of MSCs-GFP-Luci. (A) Effect of SDF-1 on surface expression of CXCR4 on MSCs-GFP-Luci detected by RT-PCR. (B) Chemotactic effect of SDF-1 on MSCs-GFP-Luci. The number of migrated MSCs increased dose-dependently at the concentration of 10-200 ng/ml SDF-1 ($P<0.05$), compared with control. The maximum effect of SDF-1 was observed at the concentration of 200 ng/ml. (C) The specificity of the effect of SDF-1 on the migration of MSCs-GFP-Luci.

When AMD3100 inhibited CXCR4 on MSCs, the chemotactic effect of SDF-1 on MSCs was abolished. Control or 0 showed the “spontaneous” migration capacity of MSCs in the presence of medium along. Data are presented as mean±SD, *P<0.05 vs control. Scale bars=25 μm (A).

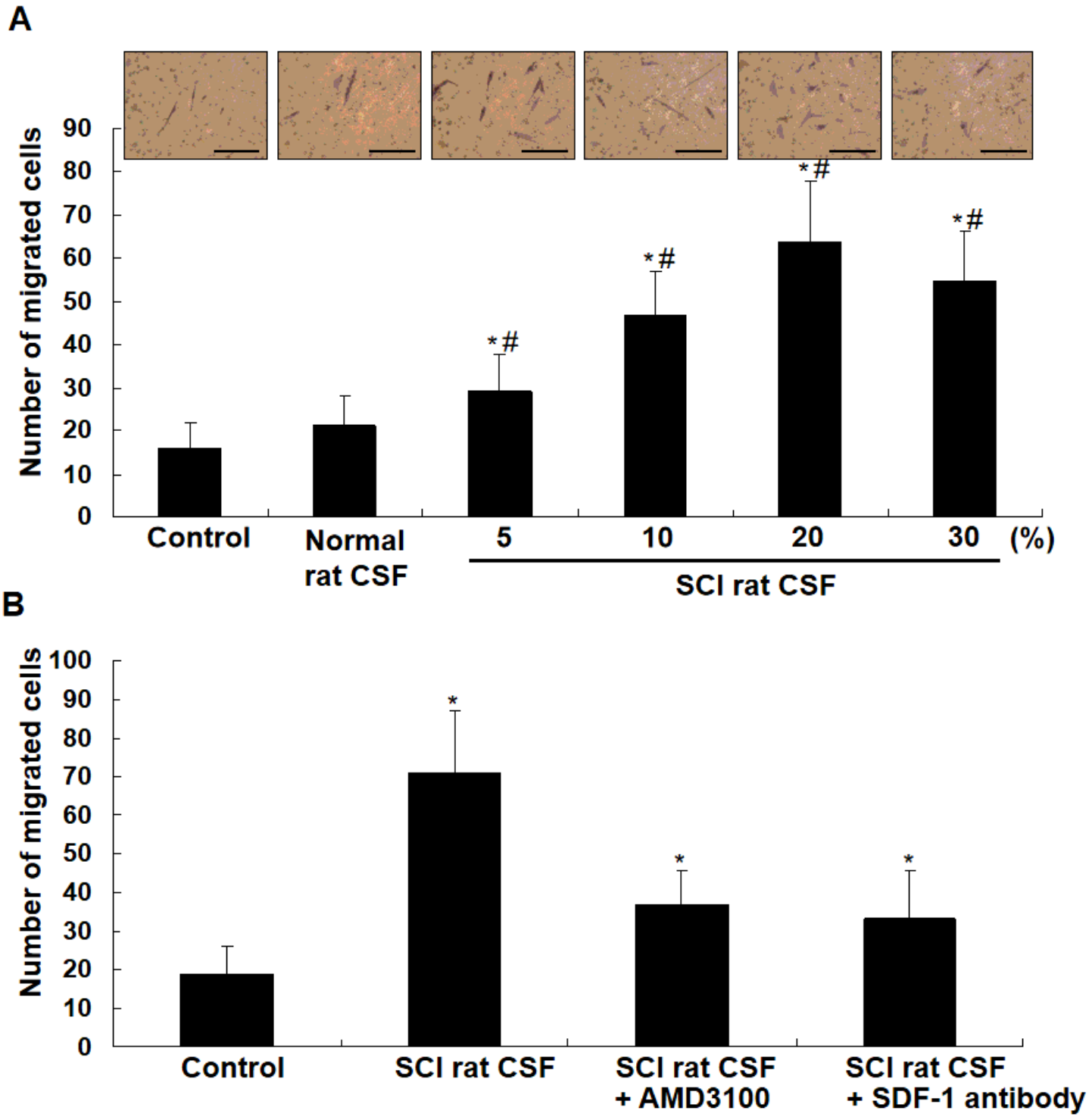

Figure 8

Effect of CSF collected from SCI rats on the migration of MSCs-GFP-Luci. (A) Chemotactic effect of CSF from SCI rats on MSCs-GFP-Luci. The number of migrated MSCs increased dose-dependently at the

concentration of 5-20% CSF from SCI rats ($P<0.05$), compared with control and CSF from normal rats. The significant chemotactic activity was observed at 20% of CSF. (B) The specificity of the effect of SDF-1 on the migration of MSCs-GFP-Luci. When CXCR4 on MSCs was inhibited by AMD3100 or SDF-1 was blocked by SDF-1 antibody (450μg/ml), the chemotactic effect of CSF from SCI rats was significantly abrogated. The control showed the “spontaneous” migration capacity of MSCs in the presence of medium along. Data are presented as mean±SD, *$P<0.05$ vs control, #$P<0.05$ vs normal CSF. Scale bars=25 μm (A).